Published in final edited form as:
J Immunol. 2013 July 1; 191(1): 407–414. doi:10.4049/jimmunol.1103779.

Myeloid Hypoxia-Inducible Factor-1α Is Essential for Skeletal Muscle Regeneration in Mice

Nina Scheerer[*], **Nathalie Dehne**[†], **Christian Stockmann**[*], **Sandra Swoboda**[*], **Hideo A. Baba**[‡], **Agnes Neugebauer**[*], **Randall S. Johnson**[§], and **Joachim Fandrey**[*]

[*]Institut für Physiologie, Universität Duisburg-Essen, D-45122 Essen, Germany

[†]Institute of Biochemistry I, Goethe-University Frankfurt, D-60590 Frankfurt, Germany

[‡]Institut für Pathologie und Neuropathologie, Universitätsklinikum Essen, D-45122 Essen, Germany

[§]Department of Physiology, Development and Neuroscience, University of Cambridge, Cambridge CB2 3EG, United Kingdom

Abstract

The outstanding regeneration ability of skeletal muscle is based on stem cells that become activated and develop to myoblasts after myotrauma. Proliferation and growth of myoblasts result in self-renewal of skeletal muscle. In this article, we show that myotrauma causes a hypoxic microenvironment leading to accumulation of the transcription factor hypoxia-inducible factor-1 (HIF-1) in skeletal muscle cells, as well as invading myeloid cells. To evaluate the impact of HIF-1 in skeletal muscle injury and repair, we examined mice with a conditional HIF-1α knockout targeted to skeletal muscle or myeloid cells in a model of soft tissue trauma. No differences in acute trauma size were detected between control and HIF-1α knockout mice. However, muscles of myeloid HIF-1α knockout mice showed a significant delay in myoblast proliferation and growth of regenerating myofibers, in association with decreased expression of cyclooxygenase-2 in HIF-1α–deficient myeloid cells. Moreover, the removal of necrotic cell debris and the regeneration of endothelial cell structure were impaired in myeloid HIF-1α knockout mice that showed delayed invasion of macrophages to the injury site. Our findings for the first time, to our knowledge, demonstrate that myeloid HIF-1α is required for adequate skeletal muscle regeneration.

Skeletal muscle has an outstanding ability for repair after different types of injury, such as contusion or laceration, even after severe damage. The regenerative capacity is mainly based on stem cells, also known as satellite cells (SCs), located between the myofiber sarcolemma and the basal membrane. Myotrauma releases SCs from their normally quiescent state, activating proliferation and leading to self-renewal. SCs will ultimately differentiate into

Address correspondence and reprint requests to Prof. Joachim Fandrey, Institut für Physiologie, Universität Duisburg-Essen, Hufelandstrasse 55, D-45122 Essen, Germany. joachim.fandrey@uni-due.de.
This work was supported by a grant from the Deutsche Forschungsgemeinschaft.

Disclosures
The authors have no financial conflicts of interest.

Europe PMC Funders Author Manuscripts

multinucleated myofibers. The repair process generally consists of three overlapping phases, each of which is characterized by complex interactions between skeletal muscle and immune cells. Skeletal muscle cells become necrotic during the destruction phase, and neutrophils recruited to the area promote further damage by NO-mediated cell lysis. SCs proliferate, differentiate, and form multinucleated myofibers during the repair phase. Macrophages phagocytize necrotic cell debris and promote repair of the muscle as well as vasculature by direct cell–cell contacts and the release of growth factors like vascular endothelial growth factor (VEGF), hepatocyte growth factor (HGF), and PGs (1–6). Muscle regeneration is completed by maturation and contraction of myofibers during the remodeling phase (2, 6).

Severe muscle damage destroys the vasculature at the injury site, reducing blood flow and consequently oxygen supply to the injury site. The ratio of oxygen demand to oxygen supply is further increased by the influx of immune cells that consume large amounts of oxygen. Cells rapidly respond to hypoxic and inflammatory environments by upregulating gene expression under control of the transcription factor hypoxia-inducible factor (HIF) (7, 8). HIF consists of a hypoxia-inducible α-subunit and a constitutively expressed β-subunit localized to the nucleus. Under normoxic conditions, specific HIF-α prolyl-hydroxylase domain–containing enzymes hydroxylate the α-subunit in an oxygen-dependent manner. Prolyl-hydroxylated HIF-α is recognized by the von Hippel–Lindau gene product pVHL, which forms a complex with the E3 ubiquitin ligase to polyubiquitinate HIF-α. Polyubiquitinated HIF-α is rapidly degraded by the proteasome (9). Under hypoxia, HIF-α protein is stabilized, accumulates, and is then translocated into the nucleus, where it dimerizes with the β-subunit. The HIF heterodimer binds to hypoxic response elements in regulatory DNA domains of hypoxia-inducible genes and induces their transcription (10). Inflammation also increases expression of the HIF α-subunit, either by inducing transcription or translation depending on the type of inflammatory stimulus (8).

In skeletal muscle injury, skeletal muscle and myeloid cells need to adapt to hypoxia and inflammation. Conditional deletion of HIF-1α in skeletal muscle and myeloid cells in mice has revealed an important role for HIF-1α in metabolic control of muscle function and in migratory, invasive, and phagocytic macrophage functions, respectively (7, 11–14). In this study, we set out to investigate the impact of HIF-1α in skeletal muscle, as well as myeloid cells on skeletal muscle injury and repair, using a model of soft tissue trauma of the mouse hind limb in mice with a conditional HIF-1α knockout targeted to skeletal muscle and myeloid cells, respectively.

Materials and Methods

Transgenic mice

Cell-specific knockout of HIF-1α was achieved by breeding C57BL/6J mice with both alleles of exon 2 of HIF-1α flanked by *loxP* sites (HIF-1α$^{+f/+f}$) with mice expressing Cre recombinase either driven by the lysozyme M promoter (LysMCre^{+}/HIF-1α$^{+f/+f}$) or by the MCK promoter (MCKCre^{+}/HIF-1α$^{+f/+f}$) (7, 14). Mice negative for Cre recombinase with HIF-1α floxed (HIF-1α$^{+f/+f}$) served as control mice. Genotyping was performed by amplification of genomic DNA extracted from ear punches using the Taq Polymerase Kit

(Promega) and the specific primers (Table I). Mice with a conditional VEGF knockout in myeloid cells were generated and genotyped as described before (15).

Animals were kept and treated in accordance with the German law for animal welfare and institutional regulations for animal handling. Experimental procedures were approved by the Landesamt für Natur, Umwelt und Verbraucherschutz Nordrhein-Westfalen (LANUV NRW).

Procedure of myotrauma

Closed muscle trauma to the mouse hind limb was induced by using a dropmass technique from a rat model by Crisco et al. (16) with modifications as described previously (17). Under analgesia with buprenorphine (0.1 mg/kg body weight) and general anesthesia with ketamine/xylazine, a 69.2-g weight was dropped from a height of 51.6 cm onto a metal piston with a surface of 1 cm^2 placed above the gastrocnemius muscle (standardized impact energy E = 0.35 J). Both gastrocnemius muscles were injured one after the other. The trauma did not cause any bone fractures. Triceps muscles served as noninjured control muscles.

Blood and muscle tissue sampling

At 3, 24, 48, 168, or 240 h after trauma, mice were anesthetized with isoflurane and blood samples were collected via puncture of the retro-orbital venous plexus with a noncoated capillary (Sarstedt). Afterward, animals were sacrificed by cervical dislocation, and both traumatized gastrocnemius muscles with adherent soleus muscle and control triceps muscles were harvested. The tissue was either transferred into 4% paraformaldehyde or snap-frozen in liquid nitrogen and stored at −70°C until analysis. The blood serum was separated immediately by centrifugation at 10,000 rpm for 10 min and stored at 4°C until analysis.

Creatine kinase serum levels

Creatine kinase (CK) was determined in the central laboratories of the University Clinics Essen using a commercially available assay (AVIDA Systems, Bayer HealthCare).

RNA preparation and RT-PCR

Total RNA was isolated by the acid guanidinium thiocyanate/phenol/chloroform extraction method (18). One microgram of total RNA was reverse-transcribed into cDNA with oligo$(dT)_{15}$ as primer for avian myeloblastosis virus reverse transcriptase (Promega). Real-time PCR was performed with SYBR green as fluorescent dye (Eurogentec) on the Gene Amp 5700 Sequence Detection System (Applied Biosystems). The cDNA standards for real-time PCR were prepared from the specific PCR products using a DNA purification kit (Roche). The amount of standard cDNA was determined photometrically. The standard concentrations ranged from 1000 to 0.001 fg/μl. Quantification was done in a two-step real-time PCR with a denaturation step at 95°C for 10 min and then 40 cycles at 95°C for 15 s and at 60°C for 1 min (19). Primer sequences are listed in Table I.

Immunohistochemistry

Immunohistochemistry was performed on paraformaldehyde-fixed, paraffin-embedded samples according to the manufacturer’s instructions (Vector Laboratories). As primary Abs,

rat anti-F4/80, a marker for activated mouse macrophages (Serotec) at dilution 1:100, rat anti-CD34 (Novus) at dilution 1:200, rabbit anti–HIF-1α at dilution 1:10,000, rabbit anti–inducible NO synthase (iNOS) at 1:20,000 (Enzo Life Sciences), and rabbit anti–YM-1 at dilution 1:400 (Stemcell Technologies) were used. For immunostaining with rat primary Abs, biotinylated anti-rat IgG (Santa Cruz) was used as the secondary Ab at dilution 1:200. For detection of HIF-1α, a catalyzed signal amplification system (Dako) was used. Specific staining was visualized by incubation with 3′,3′-diaminobenzidine (Vector Laboratories). Hematoxylin was used for counterstaining.

Immunofluorescent double staining

Immunofluorescence was performed on paraformaldehyde-fixed, paraffin-embedded samples according to the manufacturer's instructions (Vector Laboratories). As first primary Ab, polyclonal rabbit MyoD (Acris) at dilution 1:200 was used. The signal was visualized using rabbit IgG-Alexa Fluor 568 (dilution 1:200, cross-absorbed against mouse IgG and mouse serum; Invitrogen). As second primary Ab, biotinylated mouse PCNA (BD Pharmingen) at dilution 1:500 was used (15) in combination with an M.O.M. Kit (Vector Laboratories) including specific blocking to avoid unspecific binding of the secondary Ab mouse IgG-Alexa Fluor 488 (dilution 1:200; Invitrogen). DAPI (DAKO) was used for counterstaining.

Detection of hypoxia

To detect hypoxic regions on sections of formalin-fixed, paraffin-embedded muscle tissue, we injected mice i.p. with 60 mg/kg body weight hypoxyprobe (pimonidazole HCl; hpi Hypoxyprobe) 90 min before sacrifice. Pimonidazole forms adducts with thiol-containing proteins at $pO_2 \leq 10$ mm Hg. Adducts were detected with primary mouse anti–HP-1 (hpi Hypoxyprobe) at dilution 1:50 and an M.O.M. Kit (Vector Laboratories). Specific staining was visualized by use of streptavidin labeled with Alexa Fluor 488 (Invitrogen) at dilution 1:100. DAPI (DAKO) was used for counterstaining.

Quantitative analysis of histological markers

For quantitative distributions of histological markers within the trauma region, the whole trauma region of midline sections of muscles was photographed and saved as JPEG images that were then rearranged for a panorama view of the whole section (Autostich Program). The area of trauma was measured with the ImageJ program (National Institutes of Health, http://rsbweb.nih.gov/ij). Numbers of DAB^+ cells were counted with the ImageJ program and were related to the area of trauma. To assess the area of necrotic cells debris, we measured the area of necrotic cells with the Image J Program on H&E-stained midline sections and related them to the area of trauma. At the core of the damaged area, defined as the region that was least regenerated, the cross-sectional area (XSA) of 150 regenerating myofibers was measured with the ImageJ program to determine growth of regenerating myofibers (3). Regenerating myofibers were defined as centrally nucleated myofibers, according to myofibers that contain a recently fused myoblast.

Isolation of CD11b^{+} cells from injured skeletal muscle and FACS analysis

Myotrauma was performed as described earlier. For isolation of myeloid cells, both gastrocnemius and soleus muscles were removed and incubated in lysis buffer (DME-Medium [Life Technologies] with 3 mg/μl collagenase [Sigma-Aldrich] and 1 U/ml DNAse [Promega]) for 30–45 min. Lysis stop buffer contained DME-Medium with 10% FCS (Biochrom). Digested cells were passed through a 40-μm nylon mesh (BD Falcon) to achieve a single-cell suspension that was treated once with erythrocyte lysis buffer. The purity of isolated cells was tested by FACS analysis with a CD11b-Ab from BD Biosciences (dilution 1:200; Supplemental Fig. 3A). HIF-1α knockout efficiency was checked by real-time PCR (Supplemental Fig. 2B).

Statistics

Statistical significance of differences was calculated by one-way ANOVA and Newman–Keuls posttest or Student *t* test, respectively. The *p* values are indicated as follows: $*p \leq 0.05$, $**p \leq 0.01$, $***p \leq 0.001$.

Results

Injury sites of traumatized skeletal muscle show hypoxia and increased HIF-1α accumulation

To determine whether HIF-1α might play a role in our model of soft tissue trauma of the mouse hind limb, we first tested the hypothesis whether hypoxia-induced accumulation of HIF-1α can be detected during skeletal muscle injury. Pimonidazole staining was performed and evaluated by immunofluorescence to detect hypoxic regions in injured skeletal muscle. We observed hypoxic regions in skeletal muscle at 3 and 24 h after injury, suggesting that the HIF-1α protein might be stabilized during acute skeletal muscle injury (Fig. 1A). HIF-1α protein and mRNA were detected in control and injured skeletal muscle by immunohistochemistry and RT-PCR (Table I), respectively, and were both significantly increased in injured skeletal muscle (Fig. 1B, 1C). Particularly, invading myeloid cells stained positive for HIF-1α (Fig. 1B). These results show that HIF-1α is highly expressed during skeletal myotrauma and suggest that HIF-1α might affect skeletal muscle injury.

No differences in acute trauma severity were detected between HIF-1α$^{+f/+f}$ and MCKCre/HIF-1α$^{+f/+f}$ or LysMCre/HIF-1α$^{+f/+f}$ mice

To evaluate the importance of HIF-1α in skeletal muscle cells and myeloid cells for skeletal muscle injury, we examined mice with a conditional knockout of HIF-1α either targeted to skeletal muscle or myeloid cells (MCKCre/HIF-1α$^{+f/+f}$ and LysMCre/HIF-1α$^{+f/+f}$ mice, respectively) in our model of soft tissue trauma. The extent of the traumatized muscle region was quantified on histological midbelly sections and CK activity was measured in serum to determine the severity of acute myotrauma. Neither the size of the trauma lesions nor serum CK levels differed between HIF-1α$^{+f/+f}$ and knockout mice at any time until 48 h after injury (Fig. 2A–C, Supplemental Fig. 1A, 1B). These results indicate that neither skeletal muscle nor myeloid HIF-1α influence the severity of acute myotrauma.

During early regeneration, the increase in cell proliferation was significantly attenuated in muscles of LysMCre/HIF-1α$^{+f/+f}$ mice and was associated with decreased myeloid expression of regenerative growth factors

Proliferation of SCs is an early and important step in skeletal muscle regeneration (2, 6). Immunostaining for PCNA and MyoD (a marker for the myogenic lineage) revealed a significantly attenuated increase in proliferation of MyoD^{+} cells in LysMCre/HIF-1α$^{+f/+f}$ mice at 24 h after injury (Fig. 3A, 3B), whereas cell proliferation in MCKCre/HIF-1α$^{+f/+f}$ was normal. Numbers of invaded F4/80^{+} macrophages were not changed in LysMCre/HIF-1α$^{+f/+f}$ mice at this time (Fig. 3C, 4A, 4B). However, myeloid cells isolated from traumatized skeletal muscle of these mice were significantly impaired in their expression of cyclooxygenase-2 (COX-2) mRNA but showed no change in HGF mRNA expression (Fig. 3D, 3E). The deletion efficiency of HIF-1α–exon 2 was ~75% in LysMCre/HIF-1α$^{+f/+f}$ myeloid cells (Supplemental Fig. 3B). These results show that HIF-1α–deficient myeloid cells were impaired in the expression of COX-2 in association with impaired cell proliferation during early skeletal muscle regeneration.

LysMCre/HIF-1α$^{+f/+f}$ mice showed a significant defect of skeletal muscle and endothelial cell regeneration, as well as necrotic cell debris removal

To further address the question whether HIF-1α is required for skeletal muscle regeneration, we evaluated differentiation and growth of regenerating myofibers, as well as cell debris removal, in LysMCre/HIF-1α$^{+f/+f}$ and MCKCre/HIF-1α$^{+f/+f}$ mice. Whereas skeletal muscle regeneration was normal in MCKCre/HIF-1α$^{+f/+f}$ mice (Supplemental Fig. 1C), injury sites of LysMCre/HIF-1α$^{+f/+f}$ mice revealed significantly decreased XSAs of regenerating myofibers compared with HIF-1α$^{+f/+f}$ mice at 7 d after myotrauma (Fig. 5A, 5B). Measurement of the extent of necrotic cell debris at the injury site revealed significantly larger regions of necrotic cell debris on histological muscle sections of LysMCre/HIF-1α$^{+f/+f}$ mice, but not of MCKCre/HIF-1α$^{+f/+f}$ mice (Supplemental Fig. 1D) compared with those of HIF-1α$^{+f/+f}$ mice at 7 and 10 d after injury (Fig. 5A, 5C). These results show that cell proliferation and growth of regenerating myofibers, as well as cell debris removal, are significantly delayed in mice with a myeloid HIF-1α knockout and indicate that HIF-1α of myeloid cells, but not of skeletal muscle cells, is required for adequate skeletal muscle regeneration.

Vessel regeneration is closely associated with regeneration of skeletal myofibers (1). To determine whether myeloid HIF-1α is also required for endothelial cell regeneration after myotrauma, we stained endothelial cells with an Ab against CD34 and visualized them using a peroxidase reaction (Fig. 6A). Regeneration areas of HIF-1α$^{+f/+f}$ mice showed high and increasing numbers of CD34^{+} endothelial cells at 7 and 10 d after injury, whereas LysMCre/HIF-1α$^{+f/+f}$ muscles showed an attenuated increase in CD34 staining compared with HIF-1α$^{+f/+f}$ mice (Fig. 6B), indicating a distinct role for myeloid HIF-1α in skeletal muscle as well as endothelial cell regeneration after myotrauma.

HIF-1α–deficient myeloid cells showed delayed invasion to skeletal muscle injury sites

Macrophages promote survival and proliferation of myogenic cells by direct cell–cell contacts and soluble factors, respectively (4). To determine whether the impairment of

regeneration in LysMCre/HIF-1α$^{+f/+f}$ mice could be caused by inhibition of macrophage accumulation at the injury site, we visualized activated macrophages using an Ab against F4/80 and a peroxidase-based reaction (Fig. 4A). Only cells within the injury site were included into the quantification. Invaded macrophages were detected from 24 h after myotrauma at injury sites of HIF-1α$^{+f/+f}$ and LysMCre/HIF-1α$^{+f/+f}$ mice. When injury sites of HIF-1α$^{+f/+f}$ mice showed significantly increased numbers at 48 h after injury, numbers of macrophages at injury sites of LysMCre/HIF-1α$^{+f/+f}$ mice remained low, resulting in approximately three times lower numbers of F4/80^{+} macrophages in LysMCre/HIF-1α$^{+f/+f}$ mice (Fig. 4A, 4B). At 7 d after injury, injury sites of LysMCre/HIF-1α$^{+f/+f}$ mice showed high values of F4/80^{+} macrophages comparable with numbers at 48 h after injury in HIF-1α$^{+f/+f}$ mice, whereas numbers of F4/80^{+} macrophages at injury sites of the latter had already decreased again to low levels (Fig. 4A, 4B). These results indicate that HIF-1α–deficient macrophages were delayed in invasion to skeletal muscle injury sites, leading to reduced numbers of macrophages and consequently decreased capacity of phagocytosis and skeletal muscle regeneration in LysMCre/HIF-1α$^{+f/+f}$ mice.

VEGF is expressed by myeloid cells in dependence of HIF-1α (15, 20) and has been shown to promote angiogenesis, as well as endogenous muscle regeneration (1, 21). To test whether the lack of myeloid VEGF had caused the impaired regeneration of LysMCre/HIF-1α$^{+f/+f}$ skeletal muscle in our model, we examined skeletal muscle regeneration in mice with a conditional VEGF knockout in myeloid cells (LysMCre/VEGF$^{+f/+f}$ mice). Neither the extent of necrotic cell debris nor the numbers of CD34^{+} endothelial cells of LysMCre/VEGF$^{+f/+f}$ muscles differed from those of VEGF$^{+f/+f}$ mice (Supplemental Fig. 2A, 2B), indicating that the regeneration defect of LysMCre/HIF-1α$^{+f/+f}$ mice was not exclusively based on reduced myeloid VEGF expression.

The phenotype of macrophages shifts from an M1 to a M2 phenotype after muscle injury, resulting in enhanced muscle regeneration and growth (5). Because HIF-1α has been reported to influence macrophage polarization (22, 23), we addressed the question of whether the macrophage phenotype might be altered in LysMCre/HIF-1α$^{+f/+f}$ mice. Both wild-type and HIF-1α–deficient CD11b^{+} cells showed 100 times higher expression levels of the M2 marker arginase-1 than of the M1 marker iNOS (Supplemental Fig. 4A, 4B). We confirmed these data by immunohistochemistry, which revealed that most macrophages stained positive for YM-1 (T lymphocyte–derived eosinophil chemotactic factor) (24), whereas staining for iNOS was hardly detected (Supplemental Fig. 4C). These data revealed that in our model of soft tissue trauma, macrophages showed a M2 phenotype already at 24 h after injury independently of HIF-1α.

Discussion

In this study, we investigated the impact of HIF-1α on skeletal muscle injury and repair in a model of soft tissue trauma of the mouse hind limb. Using mice with a conditional HIF-1α knockout targeted to skeletal muscle or myeloid cells (7, 14), we have shown that whereas HIF-1α knockout in skeletal muscle cells neither influences the severity of acute myotrauma nor skeletal muscle regeneration, knockout of HIF-1α in myeloid cells significantly delays skeletal muscle regeneration. Because of the myotrauma, the injury site of skeletal muscle

developed a hypoxic and inflammatory environment. We detected HIF-1α accumulation in muscle and mainly in recruited myeloid cells, indicating that myeloid HIF-1α might play a role in skeletal muscle injury. These results are in accordance with our previous studies showing that damaged myofibers activate HIF-1 in neighboring myotubes and precursor myoblasts (25), and that in cells of the innate immune system, HIF-1 is upregulated by hypoxia and inflammatory mediators, preparing these cells to invade to and function in hypoxic and inflammatory tissue (8). Within the first few hours after injury, invading neutrophils can release large amounts of cytotoxic molecules that may aggravate muscle damage and increase the acute extent of the trauma (26). However, in our model, the serum CK levels and the extent of trauma lesions did not differ in mice with a myeloid HIF-1α knockout compared with wild type animals. Surprisingly, HIF-1α knockout in skeletal muscle cells did not influence the acute severity of trauma either. In contrast, Mason et al. (14) have reported that an HIF-1α knockout causes a metabolic shift from glycolysis to oxidation in skeletal muscle cells leading to extensive muscle damage in exercise trials. Our results suggest that in our model of soft tissue trauma, neither myeloid nor skeletal muscle HIF-1α influences the acute severity of trauma during the destruction phase.

Muscle regeneration is characterized by proliferation, differentiation, and growth of myoblasts, as well as phagocytosis of necrotic cell debris and vessel regeneration (2, 6). Whereas the lack of skeletal muscle HIF-1α did not show any influence on skeletal muscle regeneration, the lack of myeloid HIF-1α significantly delayed all phases of skeletal muscle regeneration. First, muscle cell proliferation was significantly impaired in mice with a myeloid HIF-1α knockout at 24 h after injury. At this time, the number of invaded HIF-1α–deficient myeloid cells was not yet reduced, but the decrease in the expression of COX-2 as detected in these cells could contribute to the impairment of cell proliferation in LysMCre/HIF-1α$^{f+/f+}$ mice. COX-2 catalyzes the synthesis of PGs (27), which are known to be essential during early skeletal muscle regeneration (3, 28) just as HGF (2). Our data are in accordance with an earlier publication that identified the COX-2 HIF-1 target gene (29). Interestingly, although HGF has also been reported to be regulated by HIF-1 (30), the expression was not changed. Second, the XSA of regenerating myofibers was significantly smaller in LysMCre/HIF-1α$^{f+/f+}$ mice compared with HIF-1α$^{f+/f+}$ mice at 7 d after myotrauma, indicating that the lack of myeloid HIF-1α impaired growth of regenerating myofibers. Third, larger areas of necrotic cell debris at injury sites of LysMCre/HIF-1α$^{f+/f+}$ mice revealed a significant defect of cell debris removal in these mice. Finally, the lack of myeloid HIF-1α also affected the regeneration of vessel structure as the number of CD34^{+} endothelial cells was significantly reduced at the injury site of LysMCre/HIF-1α$^{f+/f+}$ mice at 7 and 10 d after injury.

Aside from COX, macrophages also express VEGF in dependency of HIF-1 (20). VEGF is not only a key factor in angiogenesis, but in addition promotes skeletal muscle regeneration (31). But when we examined mice with a conditional knockout of VEGF targeted to myeloid cells in our model (15), no effect on either skeletal muscle or on endothelial cell regeneration was observed. These results document that myeloid VEGF alone is not required for angiogenesis and skeletal muscle regeneration after myotrauma. Moreover, our data do not support the notion that restoration of VEGF levels by invading macrophages is required for capillary formation and muscle regeneration (1).

Direct interactions of macrophages with myoblasts have been reported to play a central role in skeletal muscle and endothelial cell regeneration (2, 4, 32). Furthermore, myeloid cells express factors, independently from HIF-1, that promote skeletal muscle regeneration and growth (2, 6). Cramer et al. (7) have shown that loss of HIF-1α impairs myeloid cell aggregation, invasion, and motility. Subsequent work by another group revealed that the expression of β_2 integrins is HIF-1α dependent (11). In our model, HIF-1α–deficient macrophages were significantly delayed in their invasion to the traumatized region, leading to fewer numbers of activated macrophages at 48 h after injury, and consequently resulting in reduced direct cell–cell contacts of macrophages with regenerating myofibers and probably to reduced amounts of regeneration factors expressed by myeloid cells. The delay in macrophage invasion may thus be responsible for the delay in skeletal muscle growth, resulting in smaller XSAs of skeletal muscle cells in mice with an HIF-1α knockout in myeloid cells. Likewise, the reduced clearance of necrotic cell debris in LysMCre/HIF-1α $^{+f/+f}$ mice may, in part, be caused by delayed macrophage invasion, but the recently reported impairment of phagocytic function of HIF-1α–deficient macrophages will likely contribute to our observed phenotype (12, 13).

We also examined the shift in macrophage phenotype from M1 to M2 populations that normally induces the change from the proliferative stage to the differentiation phase of muscle regeneration during the period of days 2 and 4 after injury (6, 33). The shift in macrophage phenotype from M1 to M2 has been reported to be influenced by HIF-1α (23, 34). We detected mainly M2 macrophages at the injury site already 24 h after injury, independently of HIF-1α expression. This might be explained by our specific model of sterile mechanical injury, in contrast with other studies using unsterile types of skeletal muscle injury (33, 35). Moreover, our results are in accordance with the findings from Takeda et al. (34) showing that activated macrophages of C57BL/6J mice show a bias toward the M2 phenotype.

In conclusion, our results show for the first time, to our knowledge, that skeletal muscle cells do not need HIF-1α for adequate regeneration after soft tissue trauma. Our data further demonstrates that, in contrast, myeloid HIF-1α is required for macrophage invasion to the injury site, and that mice with a myeloid-specific knockout of HIF-1α exhibit defects in phagocytosis of necrotic cell debris and in the timely proliferation and growth of regenerating myofibers.

Supplementary Material

Refer to Web version on PubMed Central for supplementary material.

Acknowledgments

We thank I. Gendreitzig, A. Deichmann, E. Gottstein, and P. Freitag for technical assistance.

Abbreviations used in this article

CK	creatine kinase

COX	cyclooxygenase
HGF	hepatocyte growth factor
HIF-1	hypoxia-inducible factor-1
iNOS	inducible NO synthase
PCNA	proliferating cell nuclear Ag
SC	satellite cell
VEGF	vascular endothelial growth factor
XSA	cross-sectional area

References

1. Ochoa O, Sun D, Reyes-Reyna SM, Waite LL, Michalek JE, McManus LM, Shireman PK. Delayed angiogenesis and VEGF production in CCR2$^{-/-}$ mice during impaired skeletal muscle regeneration. Am J Physiol Regul Integr Comp Physiol. 2007; 293:R651–R661. [PubMed: 17522124]
2. Ten Broek RW, Grefte S, Von den Hoff JW. Regulatory factors and cell populations involved in skeletal muscle regeneration. J Cell Physiol. 2010; 224:7–16. [PubMed: 20232319]
3. Bondesen BA, Mills ST, Kegley KM, Pavlath GK. The COX-2 pathway is essential during early stages of skeletal muscle regeneration. Am J Physiol Cell Physiol. 2004; 287:C475–C483. [PubMed: 15084473]
4. Chazaud B, Sonnet C, Lafuste P, Bassez G, Rimaniol AC, Poron F, Authier FJ, Dreyfus PA, Gherardi RK. Satellite cells attract monocytes and use macrophages as a support to escape apoptosis and enhance muscle growth. J Cell Biol. 2003; 163:1133–1143. [PubMed: 14662751]
5. Tidball JG, Wehling-Henricks M. Macrophages promote muscle membrane repair and muscle fibre growth and regeneration during modified muscle loading in mice in vivo. J Physiol. 2007; 578:327–336. [PubMed: 17038433]
6. Tidball JG, Villalta SA. Regulatory interactions between muscle and the immune system during muscle regeneration. Am J Physiol Regul Integr Comp Physiol. 2010; 298:R1173–R1187. [PubMed: 20219869]
7. Cramer T, Yamanishi Y, Clausen BE, Förster I, Pawlinski R, Mackman N, Haase VH, Jaenisch R, Corr M, Nizet V, et al. HIF-1alpha is essential for myeloid cell-mediated inflammation. Cell. 2003; 112:645–657. [PubMed: 12628185]
8. Frede S, Berchner-Pfannschmidt U, Fandrey J. Regulation of hypoxia-inducible factors during inflammation. Methods Enzymol. 2007; 435:405–419. [PubMed: 17998066]
9. Jelkmann W. Molecular biology of erythropoietin. Intern Med. 2004; 43:649–659. [PubMed: 15468961]
10. Semenza GL. HIF-1 and mechanisms of hypoxia sensing. Curr Opin Cell Biol. 2001; 13:167–171. [PubMed: 11248550]
11. Kong T, Scully M, Shelley CS, Colgan SP. Identification of Pur alpha as a new hypoxia response factor responsible for coordinated induction of the beta 2 integrin family. J Immunol. 2007; 179:1934–1941. [PubMed: 17641060]
12. Anand RJ, Gribar SC, Li J, Kohler JW, Branca MF, Dubowski T, Sodhi CP, Hackam DJ. Hypoxia causes an increase in phago-cytosis by macrophages in a HIF-1alpha-dependent manner. J Leukoc Biol. 2007; 82:1257–1265. [PubMed: 17675562]
13. Acosta-Iborra B, Elorza A, Olazabal IM, Martín-Cofreces NB, Martin-Puig S, Miró M, Calzada MJ, Aragonés J, Sánchez-Madrid F, Landázuri MO. Macrophage oxygen sensing modulates antigen presentation and phagocytic functions involving IFN-gamma production through the HIF-1 alpha transcription factor. J Immunol. 2009; 182:3155–3164. [PubMed: 19234213]

14. Mason SD, Howlett RA, Kim MJ, Olfert IM, Hogan MC, McNulty W, Hickey RP, Wagner PD, Kahn CR, Giordano FJ, Johnson RS. Loss of skeletal muscle HIF-1alpha results in altered exercise endurance. PLoS Biol. 2004; 2:e288. [PubMed: 15328538]
15. Stockmann C, Doedens A, Weidemann A, Zhang N, Takeda N, Greenberg JI, Cheresh DA, Johnson RS. Deletion of vascular endothelial growth factor in myeloid cells accelerates tumorigenesis. Nature. 2008; 456:814–818. [PubMed: 18997773]
16. Crisco JJ, Hentel KD, Jackson WO, Goehner K, Jokl P. Maximal contraction lessens impact response in a muscle contusion model. J Biomech. 1996; 29:1291–1296. [PubMed: 8884474]
17. Kerkweg U, Schmitz D, de Groot H. Screening for the formation of reactive oxygen species and of NO in muscle tissue and remote organs upon mechanical trauma to the mouse hind limb. Eur Surg Res. 2006; 38:83–89. [PubMed: 16612092]
18. Chomczynski P, Sacchi N. Single-step method of RNA isolation by acid guanidinium thiocyanate-phenol-chloroform extraction. Anal Biochem. 1987; 162:156–159. [PubMed: 2440339]
19. Frede S, Stockmann C, Freitag P, Fandrey J. Bacterial lipopoly-saccharide induces HIF-1 activation in human monocytes via p44/42 MAPK and NF-kappaB. Biochem J. 2006; 396:517–527. [PubMed: 16533170]
20. Richard DE, Berra E, Pouysségur J. Angiogenesis: how a tumor adapts to hypoxia. Biochem Biophys Res Commun. 1999; 266:718–722. [PubMed: 10603309]
21. Deasy BM, Feduska JM, Payne TR, Li Y, Ambrosio F, Huard J. Effect of VEGF on the regenerative capacity of muscle stem cells in dystrophic skeletal muscle. Mol Ther. 2009; 17:1788–1798. [PubMed: 19603004]
22. Shirato K, Kizaki T, Sakurai T, Ogasawara JE, Ishibashi Y, Iijima T, Okada C, Noguchi I, Imaizumi K, Taniguchi N, Ohno H. Hypoxia-inducible factor-1alpha suppresses the expression of macrophage scavenger receptor 1. Pflugers Arch. 2009; 459:93–103. [PubMed: 19641936]
23. Werno C, Menrad H, Weigert A, Dehne N, Goerdt S, Schledzewski K, Kzhyshkowska J, Brüne B. Knockout of HIF-1α in tumor-associated macrophages enhances M2 polarization and attenuates their pro-angiogenic responses. Carcinogenesis. 2010; 31:1863–1872. [PubMed: 20427344]
24. Raes G, Van den Bergh R, De Baetselier P, Ghassabeh GH, Scotton C, Locati M, Mantovani A, Sozzani S. Arginase-1 and Ym1 are markers for murine, but not human, alternatively activated myeloid cells. J Immunol. 2005; 174:6561. [PubMed: 15905489]
25. Dehne N, Kerkweg U, Flohé SB, Brüne B, Fandrey J. Activation of hypoxia-inducible factor 1 in skeletal muscle cells after exposure to damaged muscle cell debris. Shock. 2011; 35:632–638. [PubMed: 21283061]
26. Tidball JG. Inflammatory processes in muscle injury and repair. Am J Physiol Regul Integr Comp Physiol. 2005; 288:R345–R353. [PubMed: 15637171]
27. Smith WL, Garavito RM, DeWitt DL. Prostaglandin endoperoxide H synthases (cyclooxygenases)-1 and -2. J Biol Chem. 1996; 271:33157–33160. [PubMed: 8969167]
28. Shen W, Li Y, Tang Y, Cummins J, Huard J. NS-398, a cyclo-oxygenase-2-specific inhibitor, delays skeletal muscle healing by decreasing regeneration and promoting fibrosis. Am J Pathol. 2005; 167:1105–1117. [PubMed: 16192645]
29. Lee JJ, Natsuizaka M, Ohashi S, Wong GS, Takaoka M, Michaylira CZ, Budo D, Tobias JW, Kanai M, Shirakawa Y, et al. Hypoxia activates the cyclooxygenase-2-prostaglandin E synthase axis. Carcinogenesis. 2010; 31:427–434. [PubMed: 20042640]
30. Chu SH, Feng DF, Ma YB, Zhu ZA, Zhang H, Qiu JH. Stabilization of hepatocyte growth factor mRNA by hypoxia-inducible factor 1. Mol Biol Rep. 2009; 36:1967–1975. [PubMed: 18979225]
31. Germani A, Di Carlo A, Mangoni A, Straino S, Giacinti C, Turrini P, Biglioli P, Capogrossi MC. Vascular endothelial growth factor modulates skeletal myoblast function. Am J Pathol. 2003; 163:1417–1428. [PubMed: 14507649]
32. Sonnet C, Lafuste P, Arnold L, Brigitte M, Poron F, Authier FJ, Chrétien F, Gherardi RK, Chazaud B. Human macrophages rescue myoblasts and myotubes from apoptosis through a set of adhesion molecular systems. J Cell Sci. 2006; 119:2497–2507. [PubMed: 16720640]
33. St Pierre BA, Tidball JG. Differential response of macrophage subpopulations to soleus muscle reloading after rat hindlimb suspension. J Appl Physiol. 1994; 77:290–297. [PubMed: 7961247]

34. Takeda N, O'Dea EL, Doedens A, Kim JW, Weidemann A, Stockmann C, Asagiri M, Simon MC, Hoffmann A, Johnson RS. Differential activation and antagonistic function of HIF-alpha isoforms in macrophages are essential for NO homeostasis. Genes Dev. 2010; 24:491–501. [PubMed: 20194441]

35. Arnold L, Henry A, Poron F, Baba-Amer Y, van Rooijen N, Plonquet A, Gherardi RK, Chazaud B. Inflammatory monocytes recruited after skeletal muscle injury switch into antiinflammatory macrophages to support myogenesis. J Exp Med. 2007; 204:1057–1069. [PubMed: 17485518]

Europe PMC Funders Author Manuscripts

Europe PMC Funders Author Manuscripts

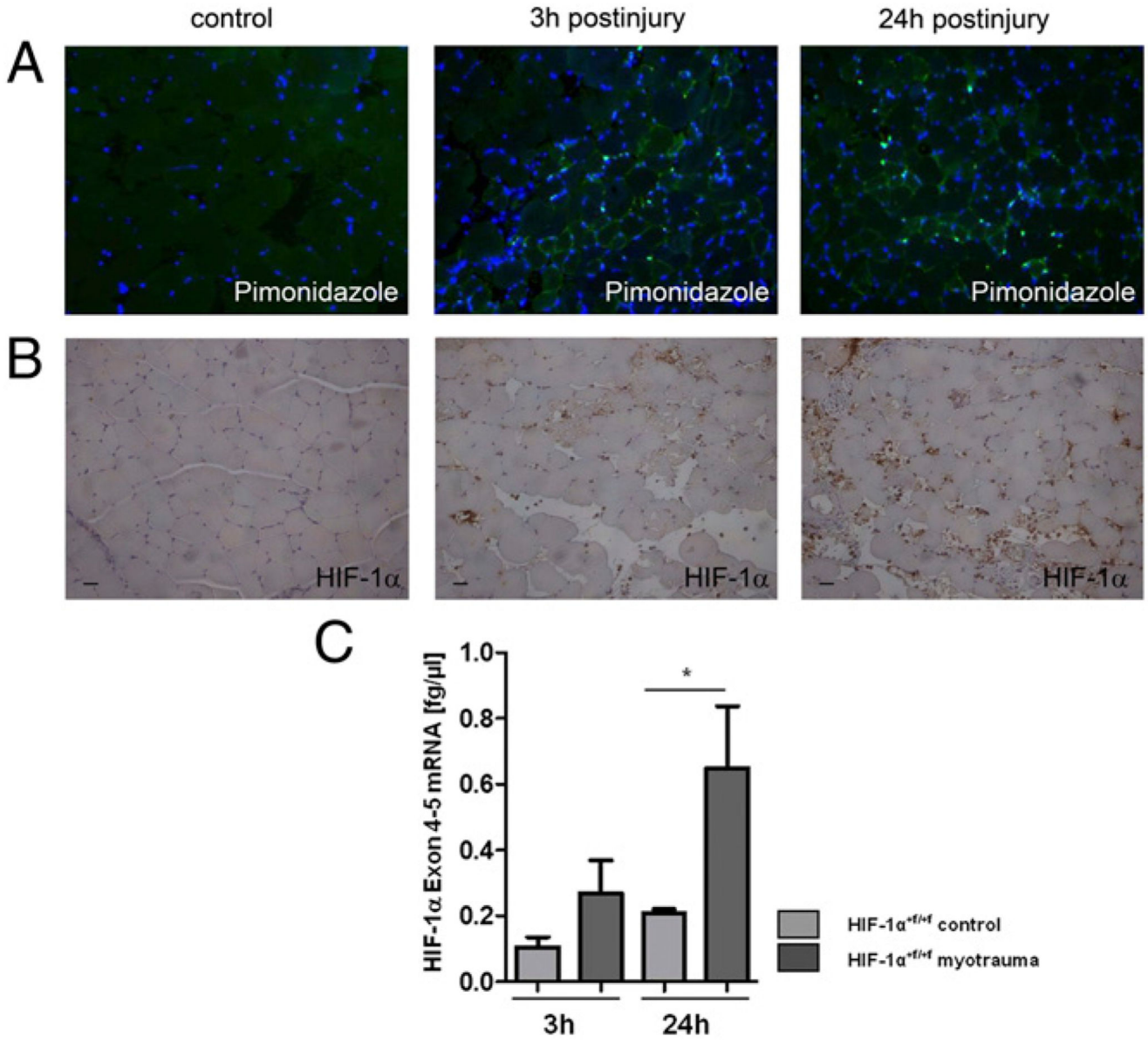

Figure 1. Injured skeletal muscle showed hypoxic regions and high HIF-1α expression.

(**A**) Representative fluorescence pimonidazole staining (green) of myofibers at 3 and 24 h after injury visualizing hypoxic regions. Counterstaining with DAPI (blue). DAPI staining increased at 3 and 24 h after injury as immune cells invaded to the injury site. $n = 4$. (**B**) Representative HIF-1α immunostaining of control and injured skeletal muscle. $n = 3$. (**C**) Quantification of HIF-1α mRNA of whole-muscle lysates of HIF-1α$^{+f/+f}$ mice. $n = 5$. Scale bars, 50 µm. *$p \leq 0.05$.

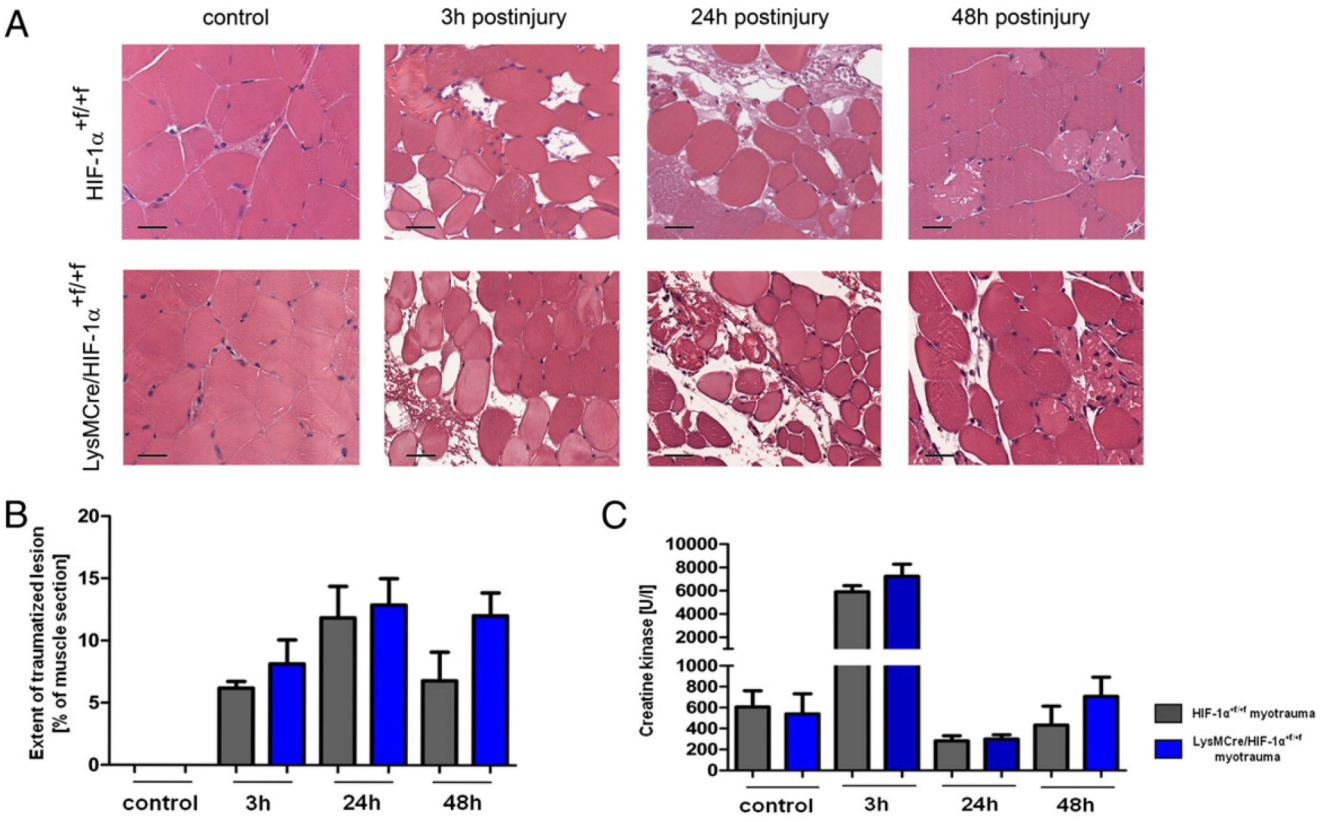

Figure 2. Muscles of HIF-1α$^{+f/+f}$ and LysMCre/HIF-1α$^{+f/+f}$ mice showed a similar severity of acute myotrauma.

(**A**) Representative histopathology (H&E staining) of control and injured muscles. (**B** and **C**) Neither the extent of traumatic lesion nor the serum CK levels differed significantly between HIF-1α$^{+f/+f}$ and LysMCre/HIF-1α$^{+f/+f}$ mice. Each group included five mice. Scale bars, 100 μm. Data are mean ± SEM.

Europe PMC Funders Author Manuscripts

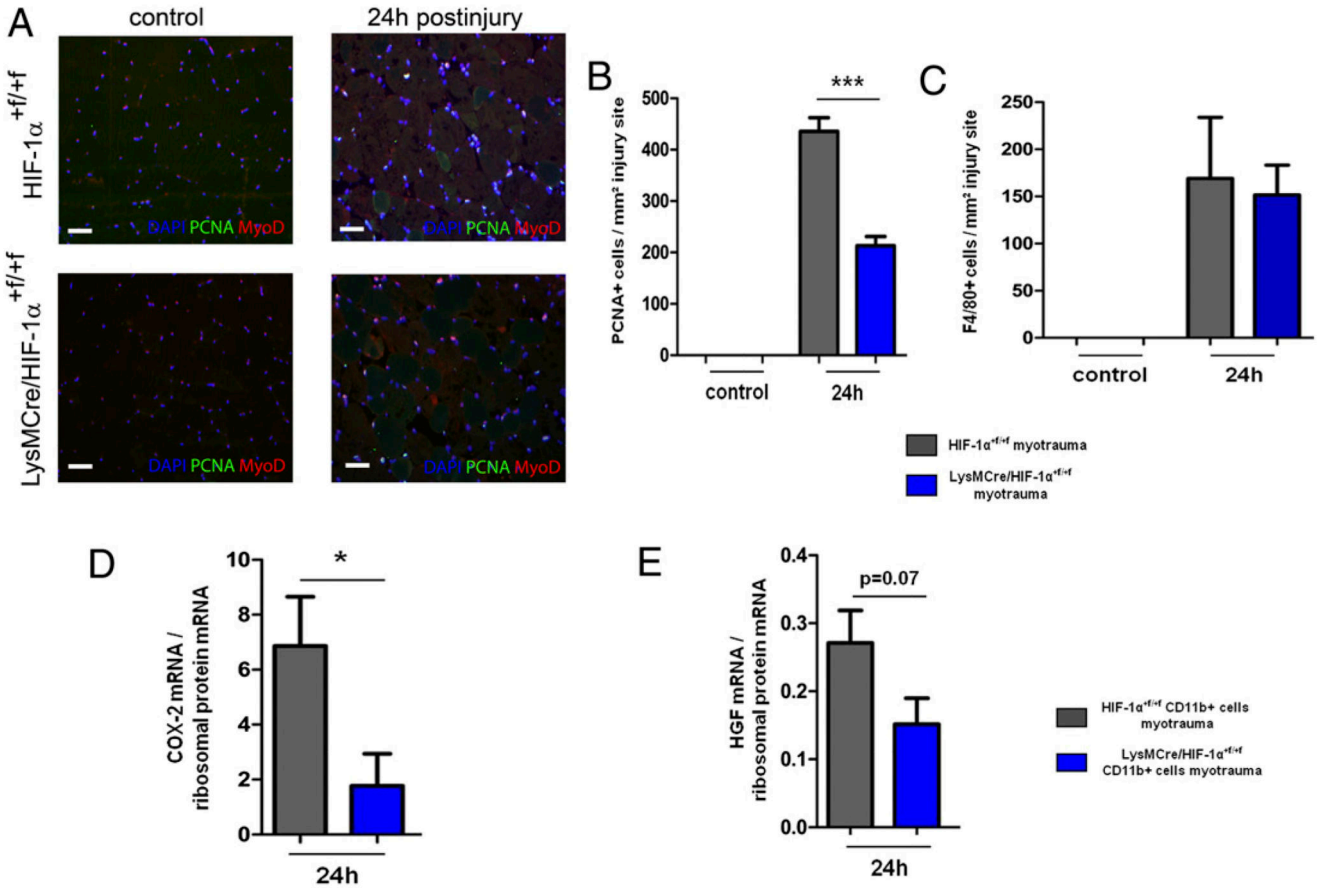

Figure 3. During early skeletal muscle regeneration, LysMCre/HIF-1α$^{+f/+f}$ mice showed an attenuated increase in proliferation of MyoD^{+} cells and decreased myeloid COX-2 and HGF expression.

(**A**) Representative immunostaining of PCNA^{+} and MyoD^{+} cells of HIF-1α$^{+f/+f}$ and LysMCre/HIF-1α$^{+f/+f}$ muscles at 24 h after injury. (**B**) Muscles of LysMCre/HIF-1α$^{+f/+f}$ mice showed a significantly attenuated increase in numbers of PCNA^{+} cells at 24 h after injury. (**C**) At 24 h after injury, the numbers of infiltrating F4/80^{+} macrophages did not differ between HIF-1α$^{+f/+f}$ and LysMCre/HIF-1α$^{+f/+f}$ mice. (**D** and **E**) COX-2 mRNA expression was decreased in HIF-1α–deficient myeloid cells isolated from injured skeletal muscle of LysMCre/HIF-1α$^{+f/+f}$ mice. Each group included four to five mice. Scale bars, 50 μm. Data are mean ± SEM. *$p \leq 0.05$, ***$p \leq 0.001$.

Europe PMC Funders Author Manuscripts

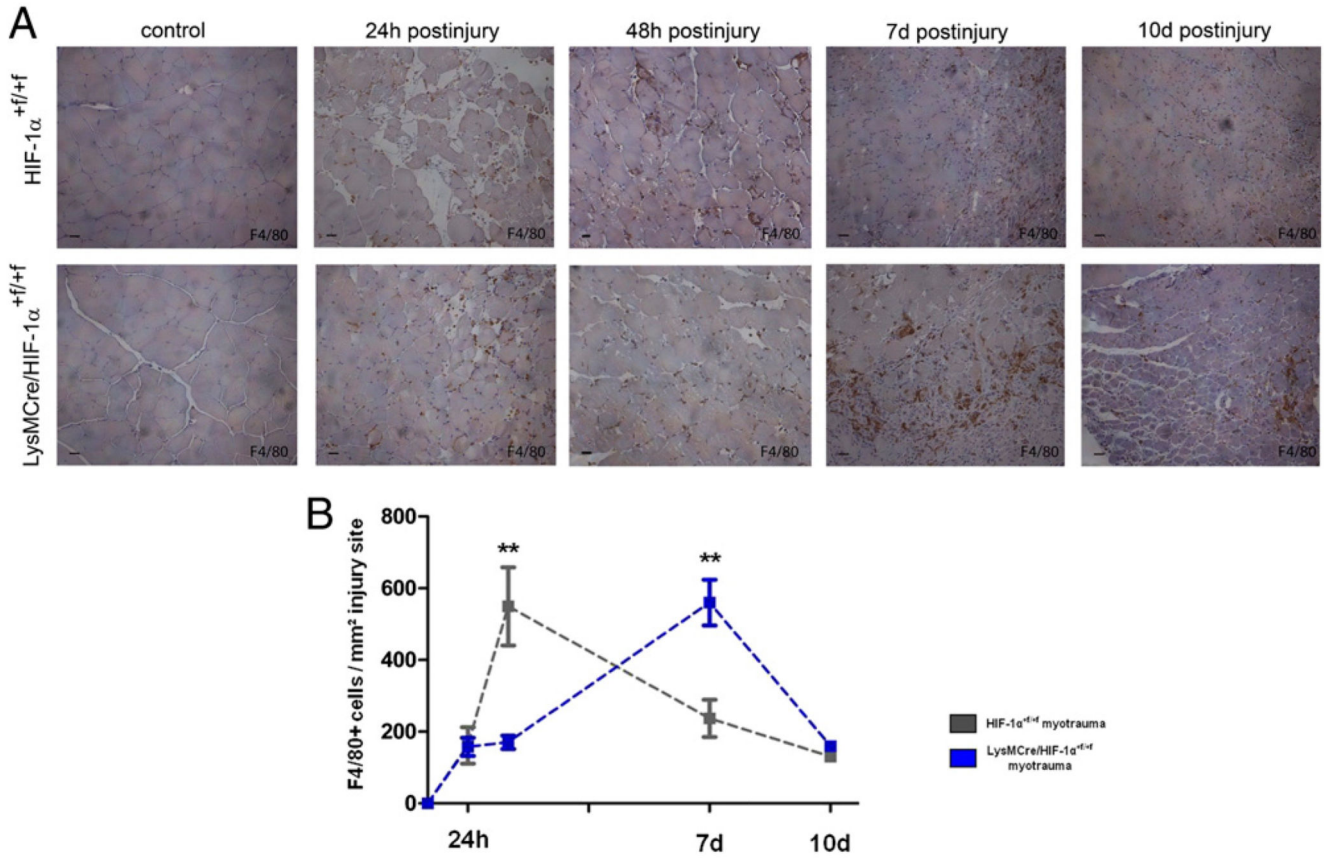

Figure 4. F4/80^{+} macrophages lacking HIF-1α were delayed in their invasion to the injury site.

(**A**) Representative F4/80 immunostaining of injured muscles of HIF-1α$^{+f/+f}$ and LysMCre/HIF-1α$^{+f/+f}$ mice. (**B**) Quantification of F4/80^{+} macrophages at the injury site revealed elevated values at 48 h after myotrauma in HIF-1α$^{+f/+f}$, but not until 7 d after myotrauma in LysMCre/HIF-1α$^{+f/+f}$ mice. Each group included five mice. Scale bars, 50 μm. Data are mean ± SEM. $^{**}p \leq 0.01$.

Europe PMC Funders Author Manuscripts

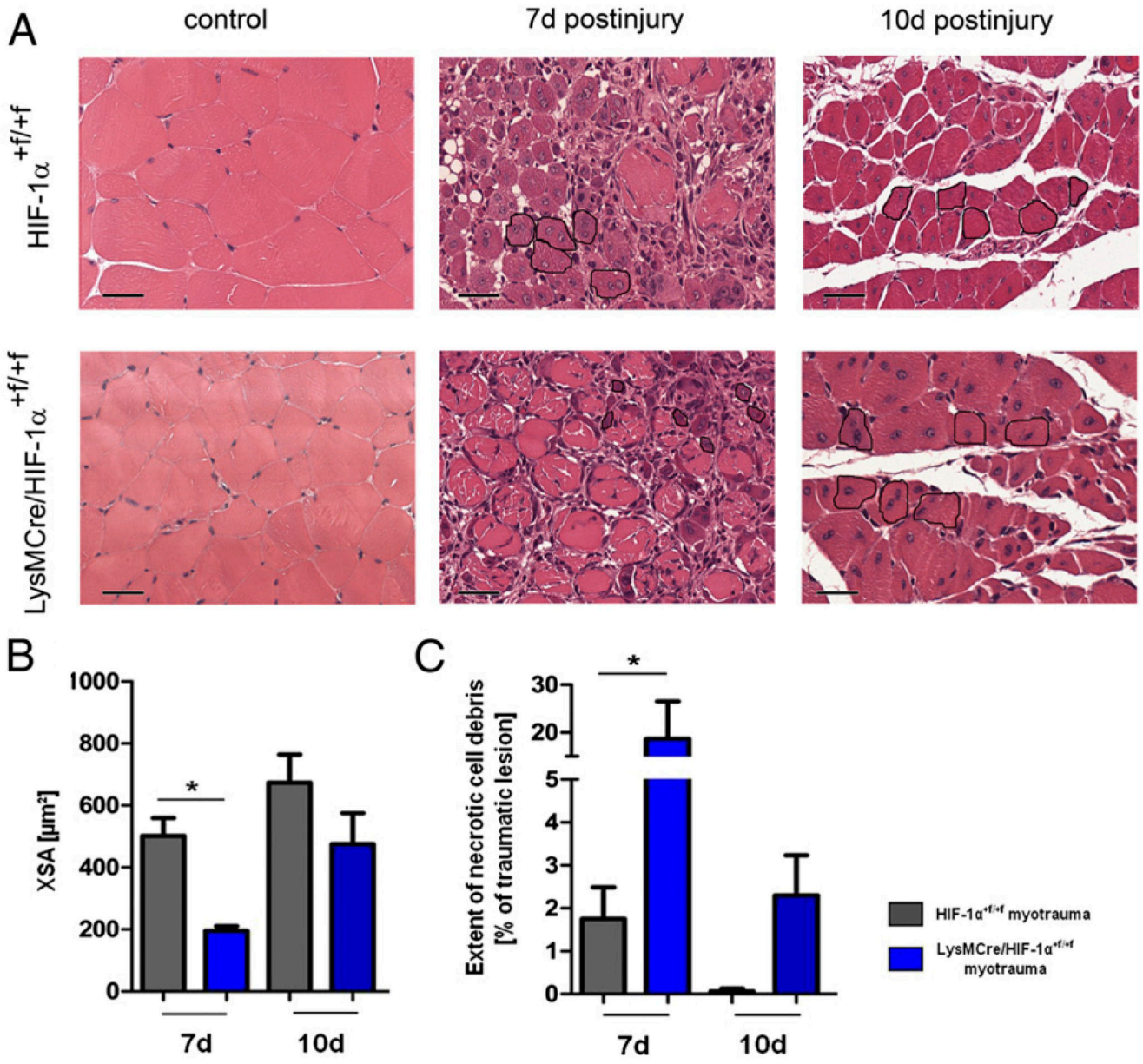

Figure 5. Muscles of LysMCre/HIF-1α$^{+f/+f}$ mice were characterized by lower XSAs of regenerating myofibers and larger areas of necrotic cell debris during the regeneration phase.

(**A**) Representative histopathology (H&E staining) at 7 and 10 d after injury. Five to six regenerating myofibers are surrounded in black to give an example how the XSA was measured. (**B**) The XSA of regenerating myofibers was significantly decreased in LysMCre/HIF-1α$^{+f/+f}$ mice. (**C**) LysMCre/HIF-1α$^{+f/+f}$ muscles showed significantly larger areas of necrotic cell debris compared with HIF-1α$^{+f/+f}$ mice. Each group included five mice. Scale bars, 100 µm. Data are mean ± SEM. *$p \leq 0.05$.

Europe PMC Funders Author Manuscripts

Europe PMC Funders Author Manuscripts

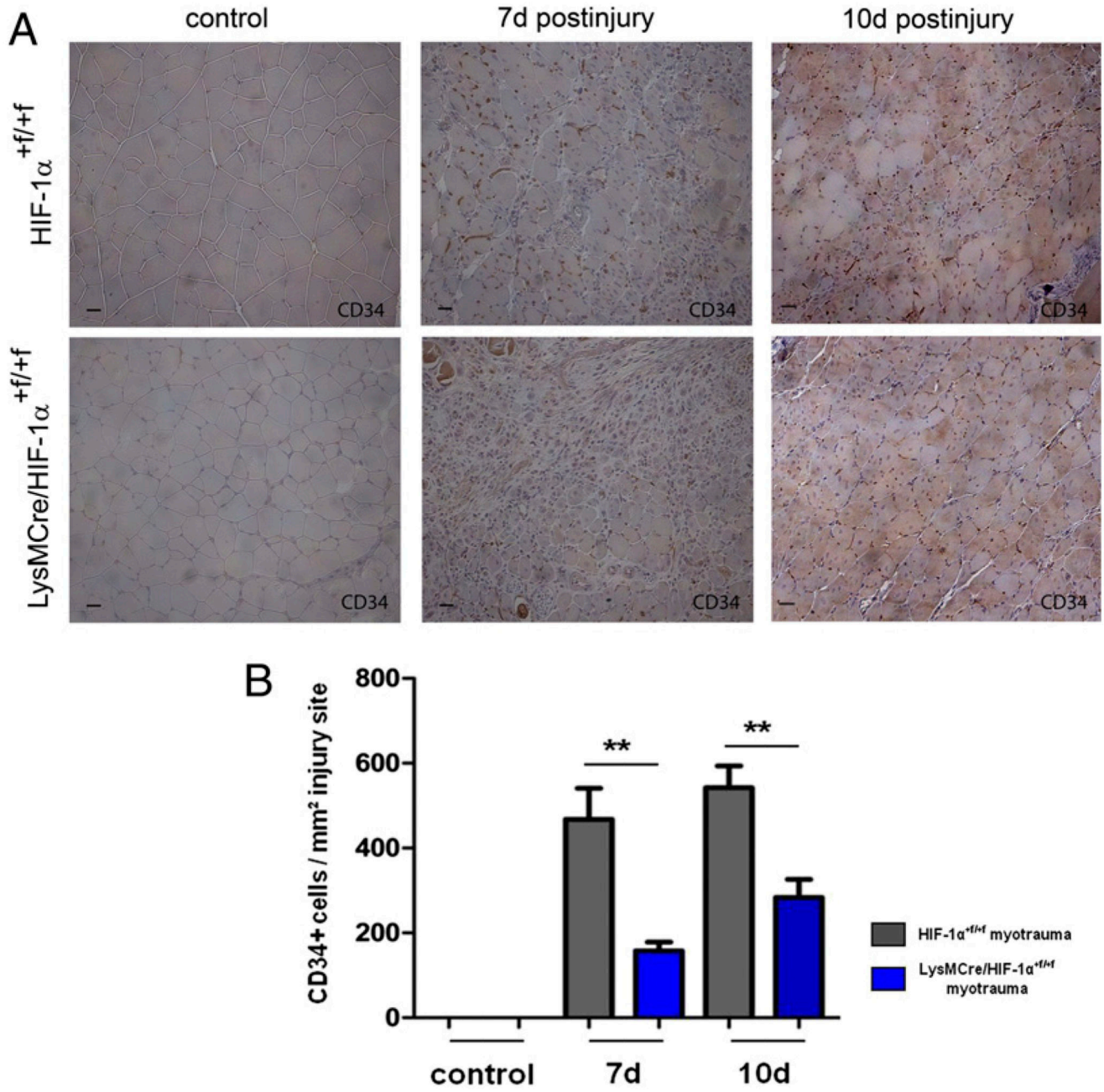

Figure 6. Numbers of CD34$^+$ endothelial cells showed a significantly attenuated increase at the injury site of LysMCre/HIF-1α$^{+f/+f}$ mice.

(**A**) Representative CD34 immunostaining of traumatized skeletal muscle at 7 and 10 d after myotrauma. (**B**) Quantification of CD34$^+$ endothelial cells revealed significantly lower numbers at LysMCre/HIF-1α$^{+f/+f}$ injury sites. Each group included five mice. Scale bars, 50 μm. Data are mean ± SEM. $^{**}p \leq 0.01$.

Table I

Primer sequences

Primer	Sequence 5′-3′
HIF-1α$^{+f/+f}$ forward primer	GGA GCT ATC TCT CTA GAC C
HIF-1α$^{+f/+f}$ reverse primer	GCA GTT AAG AGC ACT AGT
LysM-Cre forward primer	CTT GGG CTG CCA GAA TTT CTC
LysM-Cre reverse primer-1	TTA CAG TCG GCC AGG CTG AC
LysM-Cre reverse primer-2	TTA GCT GGA CCA AAT GTT GCT G
MCK-Cre forward primer	TGC AAG TTG AAT AAC CGG AAA
MCK-Cre reverse primer	CTA GAG CCT GTT TTG CAC GTT C
COX-2 forward primer	CAG GTC ATT GGT GGA GAG GT
COX-2 reverse primer	GTC GCA CAC TCT GTT GTG CT
HGF forward primer	GCT ACT CCA ACT CCC TGC TG
HGF reverse primer	TGC CAT ACA GGT AAG CCA CA
HIF-1α (Exon 4–5) forward primer	GAA ATG GCC CAG TGA GAA AA
HIF-1α (Exon 4–5) reverse primer	CTT CCA CGT TGC TGA CTT GA
HIF-1α (Exon 2) forward primer	GGC GAA GCA AAG AGT CTG AA
HIF-1α (Exon 2) reverse primer	CAT CCA GAA GTT TTC TCA CAC G